

The Luttinger liquid kink

Trinanjana Datta,¹ E. W. Carlson,¹ and Jiangping Hu¹

¹*Department of Physics, Purdue University, West Lafayette, IN 47907**

(Dated: September 4, 2018)

Spin-charge separation in the one dimensional electron gas should give rise to two peaks in the single hole spectral function. However, unambiguous detection of these two peaks has proven difficult, since the combined effects of interactions, thermal broadening, and finite experimental resolution can suppress the spin peak. Nevertheless, a telltale kink in the dispersion remains, and the systematic temperature dependence of this kink can be used to detect spin-charge separation. Although the two peaks separate at higher binding energies, interactions and temperature strongly suppress the spin peak for repulsive interactions. As a result, the measured peak will disperse with the charge velocity at high energy. This gives rise to a kink in the effective electronic dispersion as derived from measured spectral functions.

PACS numbers: 71.10.Pm, 79.60.-i, 71.27.+a

One of the most dramatic consequences of confining electrons to one spatial dimension is the prediction of spin-charge separation. That is, due to many-body interactions the electron is no longer a stable quasiparticle, but decays into separate spin and charge modes [1, 2, 3]. A direct experimental observation of spin-charge separation has proven difficult although evidence for Luttinger liquid behavior has been reported in many 1D systems, via, *e.g.*, a suppression of the density of states near the Fermi level in ropes of carbon nanotubes[4] or power law behavior in the conductance vs. temperature in edge states of the fractional quantum Hall effect[5, 6] and carbon nanotubes[7]. Until now, very limited direct evidence for spin-charge separation has been reported. Tunneling measurements later provided evidence for explicit spin-charge separation in 1D systems, via real-space imaging of Friedel oscillations using scanning tunneling microscopy on single-walled carbon nanotubes[8] and momentum- and energy-resolved tunneling between two coupled quantum wires[9], both of which observed multiple velocities indicative of spin-charge separation. More direct evidence of spin-charge separation would be to measure separate spin and charge dispersions in a single-particle spectral function.[10] Despite much effort in this area, this has only been achieved recently in an unambiguous way in the Mott-Hubbard insulator SrCuO₂. [10] Other claims of the detection of separately dispersing spin and charge peaks with ARPES[11, 12] have been overturned[13, 14], or lack independent verification of the spin and charge energy scales.[15]

Part of the difficulty in directly measuring spin and charge dispersions through measurements proportional to the single particle spectral function is that within Luttinger liquid theory, the spinon branch is muted compared to the holon branch. Finite temperature and experimental resolution only compound the problem, making direct detection of the spinon branch in, *e.g.*, angle-

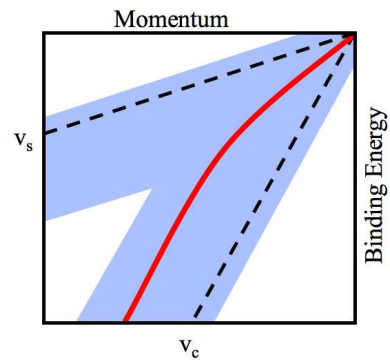


FIG. 1: (Color online) Schematic diagram of peak broadening due to interactions and finite temperature in the Luttinger liquid spectral function. The dotted lines denote the zero temperature dispersion tracking the charge part with velocity v_c and the spin part with velocity v_s . At $T \neq 0$, the peaks become thermally broadened as indicated by the shaded regions. In this case the effective dispersion now tracks the solid red line, so that the low energy part tracks the sum of the two broad spin and charge peaks, resulting in a low energy velocity v_l which is between the spin and charge velocities. Note the high energy dispersion is parallel to the charge part but displaced, an effect due to finite temperature and interactions. This results in the high energy part extrapolating back to a value $k_{ex} \neq k_F$.

resolved photoemission spectroscopy (ARPES) difficult. In this Letter, we show how spin-charge separation can nevertheless be detected via the systematic temperature dependence of a kink in the electronic dispersion, even in cases where the spin peak is not directly resolvable.

Although the electron is not an elementary excitation of the Luttinger liquid because it is unstable to spin-charge separation, an effective electronic dispersion may still be defined by the existence of (generally broad) peaks in the spectral function. At zero temperature in one dimension, there are two sharp peaks in the electronic spectral func-

*Electronic address: tdatta@physics.purdue.edu

tion, one dispersing at the velocity v_s of the collective spin modes (spinons) and the other at the velocity v_c of the collective charge modes (holons)[16, 17]. However, at finite temperature, the spin and charge peaks are broadened, as shown schematically in Fig. 1. At low binding energy, this causes the two to merge into one broad peak with a dispersion which lies between the spin velocity v_s and the charge velocity v_c . Although the two peaks separate at higher binding energies, interactions and temperature strongly suppress the spin peak for repulsive interactions. As a result, the dominant (and most easily measurable) peak will disperse with the charge velocity at high energy. This gives rise to a kink in the effective electronic dispersion. Since the Luttinger liquid is quantum critical, the kink energy scales linearly with temperature, $E_{\text{kink}} \propto a(r, \gamma_c)T$, where a is a function of the velocity ratio $r = v_s/v_c$ and the interaction strength $\gamma_c = \frac{1}{8}(K_c + K_c^{-1} - 2)$ where K_c is the charge Luttinger parameter. For $\gamma_c = 0.15 - 0.30$ and $r = 0.2 - 0.4$, the range of a is $a = 3.3 - 3.9$. The kink is stronger for lower values of r , but diminishes again for strong enough interaction strength. Moreover, the high energy linear dispersion extrapolates to the Fermi energy at a wavevector $k_{ex} \neq k_F$ which is shifted from the Fermi wavevector by an amount which scales linearly with temperature. Recently explicit analytic expressions for correlation functions in the Tomonaga-Luttinger liquid at finite temperature were obtained under various conditions[18]. We consider here the single hole spectral function, $A^<(k, \omega)$, since it is directly proportional to the intensity observed in ARPES experiments. In the spin-rotationally invariant case, the finite-temperature single hole spectral function[18] may be written in terms of the scaled variables $\tilde{k} = \frac{v_s k}{\pi T}$ and $\tilde{\omega} = \frac{\omega}{\pi T}$ with the Boltzmann constant $k_B = 1$,

$$A^<(\tilde{k}, \tilde{\omega}) \propto \int_{-\infty}^{\infty} dq h_{\frac{1}{2}}(\tilde{k} - 2rq) \times h_{\gamma_c + \frac{1}{2}} \left[\frac{\tilde{\omega} - \tilde{k}}{2} + (1+r)q \right] h_{\gamma_c} \left[\frac{\tilde{\omega} - \tilde{k}}{2} - (1-r)q \right] \quad (1)$$

where $r = v_s/v_c$ is the ratio between the spin velocity and the charge velocity and h_γ is related to the beta function,

$$h_\gamma(k) = \Re e \left[(2i)^\gamma B \left(\frac{\gamma - ik}{2}, 1 - \gamma \right) \right]. \quad (2)$$

The charge interaction strength γ_c is related to the charge Luttinger parameter K_c by $\gamma_c = \frac{1}{8}(K_c + K_c^{-1} - 2)$, *i.e.* $\gamma_c = 0$ in the noninteracting case, and γ_c increases with increasing interaction strength. Because of spin rotation invariance, we use $K_s = 1$ and $\gamma_s = 0$.

In order to define a single-hole dispersion, we use momentum distribution curves (MDC's), *i.e.* the single hole spectral function $A^<(k, \omega_o)$ considered as a function of k at a given value of the frequency ω_o . The dispersion is identified by the position $k_o = k_o(\omega_o)$ of the maximum

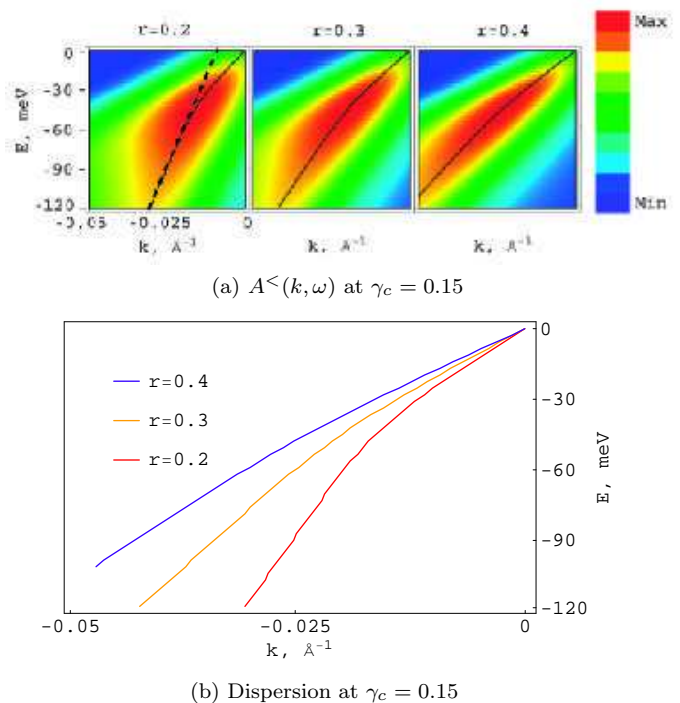


FIG. 2: (Color online) Intensity of the spectral function $A^<(k, \omega)$ and effective dispersions at an interaction strength $\gamma_c = 0.15$. (a) The intensity of $A^<(k, \omega)$ is shown for three different ratios of the spin to charge velocity, $r = 0.2, 0.3$, and 0.4 . The black lines are the effective electronic dispersions derived from MDC peaks, as described in the text. The dashed line in the first panel shows that the high energy part of the dispersion does not extrapolate back to the Fermi wavevector, k_F . (b) Comparison of the dispersions at different values of the velocity ratio, $r = 0.2, 0.3$, and 0.4 . In all cases the spin velocity $v_s = 1\text{eV}\cdot\text{\AA}$ and the temperature $k_B T = 14\text{meV}$.

of $A^<_{\text{max}}(k, \omega_o)$ with respect to k . This gives an implicit equation for the effective single hole dispersion $\omega_o(k_o)$. This method gives a more reliable definition of the effective dispersion than using energy distribution curves (EDC's), *i.e.* the spectral function considered as a function of frequency at a given momentum k_o , $A^<(k_o, \omega)$. Whereas EDC's can become quite broad with increasing interaction strength, MDC's are always sharp due to kinematic constraints,[19] so that there is less experimental uncertainty in identifying the location of a peak in the MDC.

Fig. 2(a) shows representative intensity plots of the spectral function, $A^<(k, \omega)$. In the figure, we have used an interaction strength $\gamma_c = 0.15$, temperature $k_B T = 14\text{meV}$, and velocity ratios $r = 0.2, 0.3$, and 0.4 . Fig 3 shows the corresponding MDC's for $r = 0.2$, plotted as a function of momentum k at a few representative energies. The red triangles show the position of the maximum of

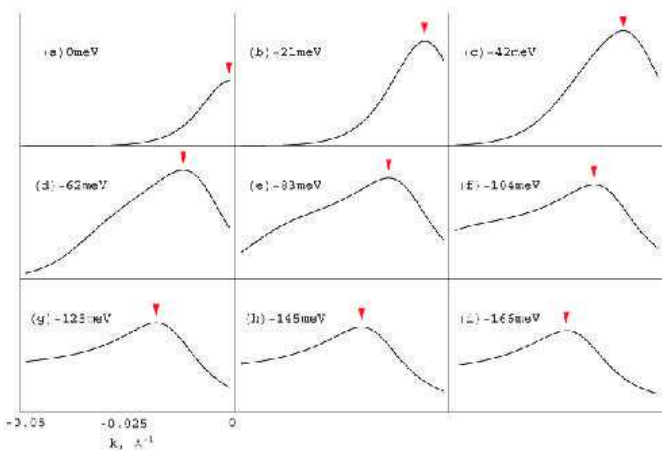


FIG. 3: (Color online) MDC's for $\gamma_c = 0.15$. The spin velocity $v_s = 1\text{eV}\cdot\text{\AA}$ and the temperature $k_B T = 14\text{meV}$. The ratio of spin to charge velocity is $r = 0.2$.

the MDC curves. The resulting effective dispersion is denoted by the solid black lines in Fig. 2(a). As is evident from the figure, the dispersion is linear as expected at low energy and also at high energy, but with different velocities. This gives rise to a “kink” in the dispersion, *i.e.* a change in the effective velocity. While at zero temperature, there are two well-defined peaks in the MDC's, one dispersing with the charge velocity and the other with the spin velocity, when the temperature is finite, the width of these MDC peaks is thermally broadened. (See Fig. 1.) At low energies and finite temperatures, the sum of the two broad peaks is itself one broad peak, as can be seen in panels (a)-(c) in Fig. 3, and the maximum in the MDC will track a velocity v_l which is between the spin and charge velocities, $v_s < v_l < v_c$. At high enough energies, the temperature broadened singularities due to the spin and charge part become sufficiently separated, and the spin peak is sufficiently muted, that the MDC peak tracks the charge velocity. The separation of the muted spin peak from the stronger charge peak can be seen in panels (d) and (e) of Fig. 3. In panels (f)-(i), the charge and spin peaks have moved sufficiently apart that the peak in the MDC will track the charge part. Aside from the presence of a kink in the effective dispersion, the position of the high energy linear dispersion is another signature of Luttinger liquid behavior. In Fig. 2(a), the dotted line is an extrapolation of the high energy linear part of the effective dispersion back to the Fermi energy. As can be seen from the figure, the dotted line extrapolates to $E = E_F$ at a wavevector $k_{ex} = k_F + \alpha(r, \gamma_c)T$ which is shifted from the Fermi wavevector by an amount which scales linearly with temperature.

Fig. 2(b) shows the effective dispersion for each of the three values of r , overlaid for comparison. As one might expect, as $r \rightarrow 1$, the kink vanishes, since then the charge and spin pieces disperse with the same velocity. As r is decreased, so that now $v_c > v_s$, a kink appears, and strengthens as r is further decreased. One can see the

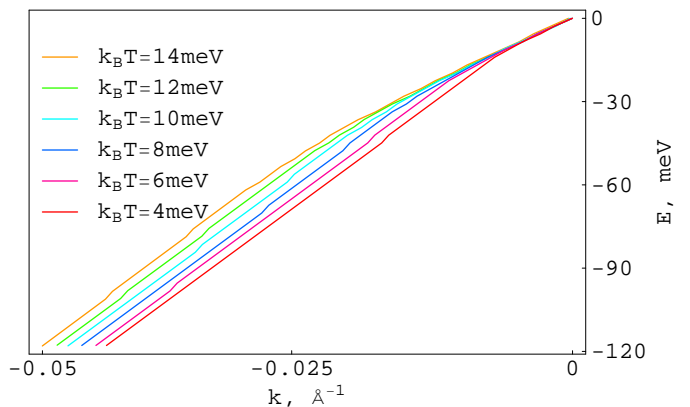


FIG. 4: (Color online) Temperature variation of the effective dispersion. The temperature varies from $k_B T = 4\text{meV}$ to $k_B T = 14\text{meV}$, starting from the lower curve and moving to the upper curve. The interaction strength $\gamma_c = 0.15$, the spin velocity $v_s = 1\text{eV}\cdot\text{\AA}$, and the ratio of spin to charge velocity $r = 0.3$.

general features that the low energy part disperses with a velocity v_l which is between the spin and charge velocities, $v_s < v_l < v_c$, and that the high energy part disperses with the charge velocity. However, this high energy dispersion extrapolates back to the Fermi energy at a wavevector $k_{ex} \neq k_F$. At higher interaction strengths, EDC's broaden significantly, so that k_{ex} is smaller and the kink diminishes in strength. However, E_{kink} moves to deeper binding energy as the interaction strength is increased.

In Fig. 4 we show how the effective dispersion changes with temperature. Because the Luttinger liquid is quantum critical, the spectral function has a scaling form, and the only energy scale in the dispersion is the temperature itself. As a result, the kink energy depends linearly on the temperature, $E_{\text{kink}} \propto T$. As can be seen in the figure, varying only the temperature merely moves the kink to deeper binding energy, leaving the low energy velocity v_l (and therefore the strength of the kink) unchanged. In addition, as temperature is increased, the high energy part extrapolates back to the Fermi energy at a higher value of k_{ex} .

Up until now, we have studied the Luttinger kink in a phenomenological manner, allowing γ_c and r to vary independently of each other. It is also useful to consider the systematics of the kink strength and energy within the context of a microscopic model. As an example, we show in Fig. 5 results for a Luttinger liquid derived from an incommensurate repulsive 1D Hubbard model. We take the density to be away from half filling, $n = 0.3$. For a given value of U/t , renormalized values of γ_c^* and r^* are taken from Ref. [20], where Bethe-ansatz was used to find the renormalized values of K_c^* , v_c^* , and v_s^* . In Fig. 5, we show the intensity plots of

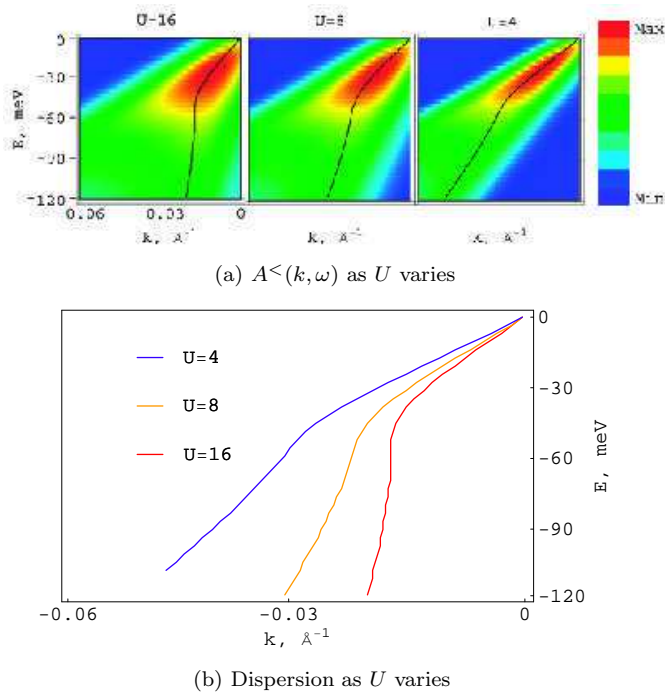


FIG. 5: (Color online) Intensity of the spectral function $A^^{less}(k, \omega)$ and effective dispersions for $U = 16, 8,$ and 4 in units of the hopping integral t . The density $n = 0.3$. (a) The intensity of $A^^{less}(k, \omega)$. The black lines are the effective electronic dispersions derived from MDC peaks, as described in the text. (b) Comparison of the dispersions at different values of U/t . In all cases the spin velocity $v_s = 1\text{eV}\cdot\text{\AA}$ and the temperature $k_B T = 14\text{meV}$.

the spectral function along with the effective dispersion, for the values $U/t = 16, 8,$ and 4 of the repulsive Hubbard model. This corresponds to renormalized values of $\gamma_c^* = 0.05, 0.04, 0.02,$ and $r^* = 0.1, 0.2, 0.4,$ respectively. Upon increasing the Hubbard interaction strength U , the strength of the kink is enhanced due to the change in the renormalized velocity ratio r^* . Notice that in this case, the kink is more pronounced, and there is a sharper distinction between the low energy and high energy linear

parts.

It is worth noting that behavior reminiscent of this physics was recently reported in ARPES experiments on the quasi-one-dimensional Mott-Hubbard insulator SrCuO_2 .^[10] Being an insulating material, SrCuO_2 is gapped, whereas the Luttinger spectral functions presented here are not. Nevertheless, the effective dispersion (measured by EDC's) shows a single peak at energies close to the gap, which then separates into two peaks at higher binding energy.

In conclusion, we have shown the existence of a temperature-dependent kink in the effective electronic dispersion of a spin-rotationally invariant Luttinger liquid, due to spin-charge separation. At low energies, the effective dispersion is linear, with a velocity between the spin and charge velocities, $v_s < v_l < v_c$. At high energies, the MDC peak disperses with the charge velocity. Because the Luttinger liquid is quantum critical, the kink between the high energy and low energy behavior has an energy set by temperature, $E_{\text{kink}} \propto T$. In addition, the high energy dispersion extrapolates back to the Fermi energy at a wavevector $k_{ex} \neq k_F$ which is shifted from the Fermi wavevector by an amount which is proportional to temperature. As interactions are increased, the kink diminishes in strength, and moves to higher binding energy. In cases where finite temperature and interactions along with experimental uncertainties obscure the detection of two separate peaks in the dispersion, the kink analysis presented here can be used as a signature of spin-charge separation in Luttinger liquids.

It is a pleasure to thank M. Grayson S. Kivelson, M. Norman, and D. Orgad for helpful discussions. This work was supported by the National Science Foundation under grant number PHY-0603759 (J.H.) and by the Purdue Research Foundation (E.W.C., T.D.). T.D. acknowledges the receipt of the Bilsland Dissertation Fellowship from Purdue University. E.W.C. is a Cottrell Scholar of Research Corporation.

[1] S. Tomonaga, *Progress of Theoretical Physics* **5**, 544 (1950).
[2] J. M. Luttinger, *Phys. Rev.* **119**, 1153 (1960).
[3] D. C. Mattis and E. H. Lieb, *Journal of Mathematical Physics* **6**, 304 (1965).
[4] M. Bockrath, D. H. Cobden, P. L. McEuen, N. G. Chopra, A. Zettl, A. Thess, and R. E. Smalley, *Science* **275**, 1922 (1997).
[5] F. P. Milliken, C. P. Umbach, and R. A. Webb, *Solid State Communications* **97**, 309 (1996).
[6] A. M. Chang, L. N. Pfeiffer, and K. W. West, *Phys. Rev. Lett.* **77**, 2538 (1996).
[7] M. Bockrath, D. H. Cobden, J. Lu, A. G. Rinzler, R. E. Smalley, L. Balents, and P. L. McEuen, *Nature* **397**, 598

(1999).
[8] J. Lee, S. Eggert, H. Kim, S.-J. Kahng, H. Shinohara, and Y. Kuk, *Physical Review Letters* **93**, 166403 (2004).
[9] O. M. Auslaender, H. Steinberg, A. Yacoby, Y. Tserkovnyak, B. I. Halperin, K. W. Baldwin, L. N. Pfeiffer, and K. W. West, *Science* **308**, 88 (2005).
[10] B. J. Kim, H. Koh, E. Rotenberg, S.-J. Oh, H. Eisaki, N. Motoyama, S. Uchida, T. Tohyama, S. Maekawa, Z.-X. Shen, et al., *Nature Physics* **2**, 397 (2006).
[11] R. Claessen, G.-H. Gweon, F. Reinert, J. W. Allen, W. P. Ellis, Z.-X. Shen, C. G. Olson, L. F. Schneemeyer, and F. Lvy, *J. Elect. Spect. Rel. Phenom.* **76**, 121 (1995).
[12] P. Segovia, D. Purdie, M. Hengsberger, and Y. Baer, *Nature* **402**, 504 (1999).

- [13] J.-L. Mozos, P. Ordejón, and E. Canadell, Phys. Rev. B **65**, 233105 (2002).
- [14] R. Losio, K. N. Altmann, A. Kirakosian, J.-L. Lin, D. Y. Petrovykh, and F. J. Himpsel, Phys. Rev. Lett. **86**, 4632 (2001).
- [15] R. Claessen, M. Sing, U. Schwingenschlögl, P. Blaha, M. Dressel, and C. S. Jacobsen, Phys. Rev. Lett. **88**, 096402 (2002).
- [16] V. Meden and K. Scönhammer, Phys. Rev. B **46**, 15753 (1992).
- [17] J. Voit, Phys. Rev. B **47**, 6740 (1993).
- [18] D. Orgad, Philos. Mag. B **81**, 375 (2001).
- [19] D. Orgad, S. A. Kivelson, E. W. Carlson, V. J. Emery, X. J. Zhou, and Z. X. Shen, Phys. Rev. Lett. **86**, 4362 (2001).
- [20] H.J.Schulz, in *Mesoscopic Quantum Physics, Les Houches LXI*, edited by E. Akkermans, G.Montambaux, J.L.Pichard, and J.Zinn-Justin (Amsterdam, Elsevier, 1995).